Biosensors and Bioelectronics 142 (2019) 111498

Contents lists available at ScienceDirect

Biosensors and Bioelectronics

journal homepage: www.elsevier.com/locate/bios

Pt–Ni(OH)$_2$ nanosheets amplified two-way lateral flow immunoassays with smartphone readout for quantification of pesticides

Nan Cheng[1], Qiurong Shi[1], Chengzhou Zhu, Suiqiong Li, Yuehe Lin, Dan Du[*]

School of Mechanical and Materials Engineering, Washington State University, Pullman, WA, 99164, USA

ARTICLE INFO

Keywords:
Smartphone
Lateral flow strip
Pt–Ni(OH)$_2$ nanosheets
Pesticides
Immunoassay

ABSTRACT

Excessive use of herbicide and insecticide causes bioaccumulation in the environment and increases potential toxicity for people and animals. Portable systems for rapid assays of herbicide and insecticide residues have attracted prominent interests. Here, we developed a two-dimensional (2D) Pt–Ni(OH)$_2$ nanosheets (NSs) amplified two-way lateral flow immunoassay (LFI) with a smartphone-based readout for simultaneous detection of acetochlor and fenpropathrin. The 2D Pt–Ni(OH)$_2$ NSs were synthesized and used as the enhanced signal label in the immunoassay due to their high peroxidase-like activity and low migration speed. The two-way LFI was designed to eliminate potential cross-reaction between two targets. Portable detection system was developed based on a smartphone-based readout, which scans the LFI and provides the accurate testing result. The universal use of smartphones makes the developed platform suitable for cheap and on-site applications. Using the integrated platform, detection of acetochlor and fenpropathrin simultaneously was successfully achieved with the detection limits of 0.63 ng/mL and 0.24 ng/mL, respectively. To confirm the performance of the on-site application, we detected 10 non-spiked samples and 3 spiked samples. The obtained detection results were consistent with the data from gas chromatography analysis. The estimated recoveries ranged from 97.12% to 111.46%, indicating the practical reliability of our developed assay. The developed smartphone-based platform exhibits enhanced sensitivity, which provides a promising technique for on-site, multiplex, highly sensitive detection of pesticides.

1. Introduction

Herbicide and insecticide are widely used in agriculture to reduce the risk of weeds and pests. However, excessive use causes bioaccumulation in the environment and increases potential toxicity for people and animals, which has been considered as a worldwide public concern (Liu et al., 2008; Kwon et al., 2017; Zhang et al., 2014). Thus, advanced pesticide detection technologies are in great demanding for the survey and control of herbicide and insecticide residues (Yan et al., 2017). Current techniques are divided into laboratory-based instrumental analysis methods and portable rapid detection techniques. Examples of instrumental analyses include gas chromatography (He et al., 2015), high performance liquid chromatography (Li et al., 2015), and mass spectrometry (Kiljanek et al., 2016), which all suffer from expensive cost, time-consuming, complex sample pretreatment, requirement of highly trained personnel, and unsuitability for on-site analysis. Thus, developing portable rapid easy-to-use technique for pesticide residue detection has attracted prominent interests.

In recent decades, lateral flow immunoassays (LFI), a promising portable rapid detection platform, has gained considerable attention due to advantages such as cost-effective, easy-to-use, and rapid-response (Ge et al., 2014; Sajid et al., 2015). Currently, LFIs for herbicide and insecticide analysis were mostly employed gold nanoparticles (AuNPs) as the signal label and designed as competitive format due to their low-molecular weight (Kim et al., 2011; Lee et al. 2012, 2013). Various LFIs have been developed to perform qualitative or semi-quantitative screening for various herbicide and insecticide, such as diazinon (Lee et al., 2012), chlorpyrifos (Kim et al., 2011), and O-ethyl O-4-nitrophenyl phenylphosphonothioate (Lee et al., 2013). Current LFIs were mainly designed to detect a single herbicide or insecticide with a specific antibody. However, to use these reported LFIs as a practical method for on-site application, three existing limitations must be overcome: (i) poor multi-detection capacity; (ii) insufficient sensitivity; and (iii) lack of simple, cheap and user-friendly readout system.

To realize simultaneous detection of multiple pesticides, LFIs, much effort has been devoted to develop single strip LFTs with more test lines.

[*] Corresponding author.
E-mail address: annie.du@wsu.edu (D. Du).
[1] These authors contribute equally.

https://doi.org/10.1016/j.bios.2019.111498
Received 22 March 2019; Received in revised form 4 July 2019; Accepted 8 July 2019
Available online 09 July 2019
0956-5663/

Take the example of double targets detection, Shu et al. developed a multiplexed LFI for detection of methyl parathion and imidacloprid using a bifunctional antibody (Shu et al., 2017). In the work published by Ouyang et al., (2018), an LFI with two test lines was developed for methyl parathion and fenpropathrin detection. However, in actual operation, the strategy of using two test lines on one LFT strip was extremely limited by uncertain consumption volume of nano-labels on the front line and unexpected interference between multiple targets and recognition molecules, which resultsg in poor analytical ability. Therefore, a multiplex LFI without cross-reaction is urgently needed.

To enhance the sensitivity of LFIs, three general methods were employed: (i) modifying the components of AuNP labels to enhance detection efficiency, such as silver enhanced AuNPs (Rong-Hwa et al., 2010), gold enhanced AuNPs (Gao et al., 2016b), silica enhanced AuNPs (Takalkar et al., 2015), horseradish peroxidase (HRP) enhanced AuNPs (Gao et al., 2016a), and G-quadruplex enhanced AuNPs (Cheng et al., 2017a), which unavoidably complicated the synthesis process; (ii) replacing AuNPs with novel labels based on different nanomaterials, such as Pt–Pd nanoparticles (Cheng et al., 2017b; Jiang et al., 2016) and Fe_3O_4 nanoparticle with 100-fold enhancement than AuNP-based LFIs (Duan et al., 2015; Zhang et al., 2017), which were mainly focus on their HRP-like activity; (iii) applying techniques to reducing the migration speed of signal labels in the LFI, such as membrane optimization (He et al., 2012), flow direction change (Park et al., 2008), and shape fabrication (Koo et al., 2013), which may bring dilemma when integrated with commercial system. These suggested that a novel LFI' label with all superior properties of high HRP-like activity, and low migration speed would be of great value.

A variety of readout platforms LFIs, including desktop readers and handheld readers have been reported in recent years. Among them, smartphone-based detection showed great potentiality in on-site applications because of the extremely broad coverage and high possession of smartphone all over the world (Roda et al., 2016). In early studies, mobile phones were only used to take pictures and send images to the lab, where a specialist can analyze the response and feedback the results (Martinez et al., 2008). Most recently, some applications (apps) were developed and pre-loaded in a smartphone, which can be applied for simple data processing on-site (Hou et al., 2017; Mudanyali et al., 2012; You et al. 2013, 2017). However, these apps were mostly designed to detect a single target. LFI platforms that achieve multiple target detection and generality applications are highly desired.

We herein report a smartphone-based device as the readout of a two-way LFI for herbicide and insecticide residue detection. Acetochlor and fenpropathrin were employed as the proof-of-concept targets in this study due to their widespread use in agriculture. Pt nanoparticles-anchored two-dimensional (2D) $Ni(OH)_2$ nanosheets (denoted as Pt–Ni $(OH)_2$ NSs) were synthesized and used as the signal enhanced label in two-way LFI with several advantageous features: i) the 2D NSs usually has a large surface area, which is beneficial for offering more catalytic active sites (Wen et al., 2018); ii) the strong interaction and synergistic effect between $Ni(OH)_2$ support and Pt nanoparticles can enhance the binding energy toward adsorption of reaction intermediates on the surface of Pt NPs and thus promoting the catalytic performances (Xu et al., 2015). These features are very desirable for LFI fabrication. Subsequently, a smartphone-based LFI analysis app was developed, which could rapidly quantify the results. This integrated strategy is potentially a valuable method for on-site detection of herbicide and insecticide.

2. Experimental section

2.1. Materials

Hydrogen peroxide (H_2O_2), 3,3′,5,5′-tetramethylbenzidine (TMB), Tween-20, K_2CO_3, sucrose, methanol, phosphate buffered saline (1 × PBS, pH 7.4, 0.01 M), and bovine serum albumin (BSA), urea, nickel nitrate, poly(methyl methacrylate (PMMA), chloroplatinic acid (H_2PtCl_6) were purchased from Sigma-Aldrich (St. Louis, MO, USA). Ethylene glycol (EG, 99%) was purchased from VWr. Nickel (II) nitrate hexahydrate (98%) was purchased from Alfa Aesar. Anti-acetochlor monoclonal antibody, anti-fenpropathrin monoclonal antibody, semiantigens of acetochlor, semiantigens of fenpropathrin, and goat anti-mouse IgG were obtained from Ditengmin Biotechnology Co., Ltd. (Wuxi, Jiangsu, China). Nitrocellulose membranes (NC membranes), sample pads, conjugate pads, backing cards, and absorbent pad were purchased from Millipore (Billerica, MA, USA).

2.2. Synthesis and characterization of 2D Pt–Ni(OH)$_2$ NSs

Pt–$Ni(OH)_2$ NSs were obtained via a two-step microwave method. In the first step, $Ni(OH)_2$ NSs were synthesized via dissolving 2 g nickel nitrate and 2 g urea in a vial containing 15 mL H_2O and 100 mL ethylene glycol. The solution was microwaved for 5 min with a power of 720 W. Subsequently, the products were washed with ethanol and water for five time, and collected through freeze drying. In the second step, the Pt–$Ni(OH)_2$ with a Pt loading amount of 20% (denoted as Pt-20/$Ni(OH)_2$) were obtained by dissolving 0.05 mmol H_2PtCl_6, 0.3 mL PMMA, and 40 mg $Ni(OH)_2$ in a vial containing 5 mL EG and 5 mL H_2O. Then the mixture was microwaved for 1 min with a power of 800 W. Then the products were washed with ethanol and water for several times. Finally, after freeze drying, the Pt–$Ni(OH)_2$ powder were obtained. Pt-10/$Ni(OH)_2$ and Pt-40/$Ni(OH)_2$ were obtained through the same procedures except the amounts of the H_2PtCl_6 used in the synthesis were 0.025 mmol and 0.1 mmol, respectively.

Transmission electron microscopy (TEM) images were obtained with a Philips CM200UT instrument. X-ray diffraction (XRD) characterization was carried out by a Rigaku Miniflex 600. Energy dispersive spectroscopy (EDS) was carried out by a JEOL-2100F electron microscope. The catalytic experiment was conducted by adding 50 μL of Pt–$Ni(OH)_2$ NSs solution,50 μL of commercial TMB and H_2O_2 mix solution in centrifuge tubes or 96-well plates. After incubating at room temperature for 5 min, the absorbance signal was observed with a Tecan Safire2 microplate reader (Tecan, Switzerland).

2.3. Preparation of antibody modified Pt–Ni(OH)$_2$ NSs conjugates

Firstly, the pH value of the Pt–$Ni(OH)_2$ NSs solution was adjusted to 8.2–8.5 using 0.02 M K_2CO_3. Then, 5 μL of anti-acetochlor antibody (1 mg/mL) or anti-fenpropathrin antibody (1 mg/mL) was added into 1 mL of Pt–$Ni(OH)_2$ NSs solution. Next, the mixture was incubated at room temperature for 60 min. After that, 10.0 wt% BSA was added to the solution and incubated at room temperature for 30 min. The resulting solution was centrifuged at 10,000 rpm for 20 min and washed with 1 × PBS containing 1% BSA for two times. Finally, the prepared antibody modified Pt–$Ni(OH)_2$ NSs conjugations were suspended in 100 μL of 1 × PBS buffer containing 2% BSA and 3% sucrose.

2.4. Preparation of two-way lateral flow strip

The two-way LFI consisted of the following components: one sample pad, two test channels for detecting acetochlor or fenpropathrin respectively, and a backing substrate. Each test channel has a NC membrane, an absorbent pad, and a test line. The test lines (1 μL/cm) were prepared by dispensing 30 μL of semiantigens of acetochlor or fenpropathrin on the NC membrane (25 mm × 30 cm) using a BioDot BioJet BJQ 3000 dispenser (Irvine, CA). Control lines (1 μL/cm) were prepared by dispensing 30 μL of goat anti-mouse IgG on the same NC membranes to maintain a 1 cm gap with test lines. The prepared NC membranes were then dried overnight at 37 °C and stored at 4 °C. The absorbent pad was assembled on backing (60 mm × 30 cm) with an overlap between them of approximately 1–2 mm to ensure that the solution could migrate through the biosensor. The two channels of the LFI with

individual test lines were assembled together by sharing the same sample pad. Assembled two-way LFIs were cut at a width of 4 mm using a Bio-Dot Paper Cutter module CM4000 (Irvine, CA).

2.5. Detection of herbicides and insecticides

In a typical test, 100 μL of diluted samples with the desired amount of targets were applied to the sample pad and migrated by capillary action. Then, the presence of acetochlor and fenpropathrin in the samples was semi-quantified by visual observation of the test line color changes after 13 min. For quantitative measurements, a smartphone (Oppo R9) with a 16-megapixel camera was used. The self-developed analysis app, named *Strip Scan*, was employed, which can provide readout of the results (unit: ng/mL) within 10 min.

2.6. Pretreatment of spiked samples

All samples except drinking water sample were purchased from Qinghe farmer market (Beijing, China). Drinking water sample was obtained from the community taps (Beijing, China). For spiked corn, apple, and cabbage samples, 1.0 g of target-free samples was homogenized to a free-flowing puree in a blender and then mixed with desired amounts of methanol dissolved acetochlor and fenpropathrin for another 2 min to ensure homogenization. Then, 10 mL of 1 × PBS containing 0.05% Tween-20 and 10% methanol were used as the elution solution to extract the spiked targets. After vortex stirring for 3 min, the mixture containing acetochlor and fenpropathrin was centrifuged at 10,000 rpm for 10 min. Finally, the supernatant was diluted to the desired volume.

3. Results and discussion

3.1. Principle of two-way LFI

The basic principle of the two-way LFI for detection of acetochlor and fenpropathrin was illustrated in Scheme 1. Briefly, were immobilized on the test lines on each test channel, respectively. The secondary antibody, goat anti-mouse IgG, was immobilized on the corresponding control lines. Anti-acetochlor antibody and anti-fenpropathrin antibody were firstly modified with Pt–Ni$(OH)_2$ NSs and then dispensed on two conjugate pads, respectively. For detection, the sample solution was applied to the sample pad and migrated by capillary action. In the absent of target (negative), the reaction between semi-antigen of acetochlor and anti-acetochlor antibody modified Pt–Ni$(OH)_2$ NSs conjugates was occurred on the left test line to form a characteristic black band. Similarly, the reaction between semi-antigen of fenpropathrin and anti-fenpropathrin antibody modified Pt–Ni$(OH)_2$ NSs conjugates was occurred on the right test line to present another black band. The remaining solution passed through the corresponding control lines, the excess anti-acetochlor antibody or anti-fenpropathrin antibody modified Pt–Ni$(OH)_2$ NSs conjugates were captured by goat anti-mouse IgG, thus two more black bands appeared on the control lines. After adding TMB and H_2O_2 mix solution on test lines, black lines turned to blue due to the HRP-like activity of Pt–Ni$(OH)_2$ NSs. In the presence of acetochlor and fenpropathrin (positive), the reactions between targets and corresponding antibody modified Pt–Ni$(OH)_2$ NSs conjugates occurred on test lines, thus created competition with the semiantigens of acetochlor and fenpropathrin on the two-way's test lines and resulted in weakened or unobservable black lines. Accordingly, the subsequent blue color change of the test lines also became weak or cannot be observed after adding TMB and H_2O_2 mix solution. Before adding TMB, the black color intensity difference of test lines between the positive and negative tests reflect the concentration of targets. However, this signal difference is very small. After adding TMB, the enhanced blue color change was obtained, which enlarged the difference between the positive and negative test lines due to the catalytic reaction between Pt–Ni$(OH)_2$ NSs and TMB/H_2O_2 mix. Because this signal enhancement strategy, this system can achieve very high sensitivity and wider the detection range effectively.

3.2. Characterization of 2D Pt–Ni$(OH)_2$ NSs

We employed TEM for the characterization of the morphologies of the as-prepared Ni$(OH)_2$ NSs with different Pt loading values (denoted as Pt-x/Ni$(OH)_2$, x represents Pt loading percentage). TEM images in Fig. 1A and B showed the typical layered Ni$(OH)_2$ NSs with wrinkles. Fig. 1C–H exhibited the uniform distribution of Pt nanoclusters on Ni$(OH)_2$ NSs. The insets in Fig. 1C, E and 1G displayed the size distributions of Pt-10/Ni$(OH)_2$, Pt-20/Ni$(OH)_2$ and Pt-40/Ni$(OH)_2$ with sizes of 2.2 ± 0.5 nm, 2.0 ± 0.5 nm and 1.8 ± 0.5 nm, respectively.

XRD was also conducted for further analyzing the structures of the Pt-x/Ni$(OH)_2$, as shown in Fig. S1A, where the diffraction peaks of typical (111), (200), (300), (220) of face-centered cubic Pt nanocrystals (PDF#04-0802) could be obviously observed. The peak of (001), (002),

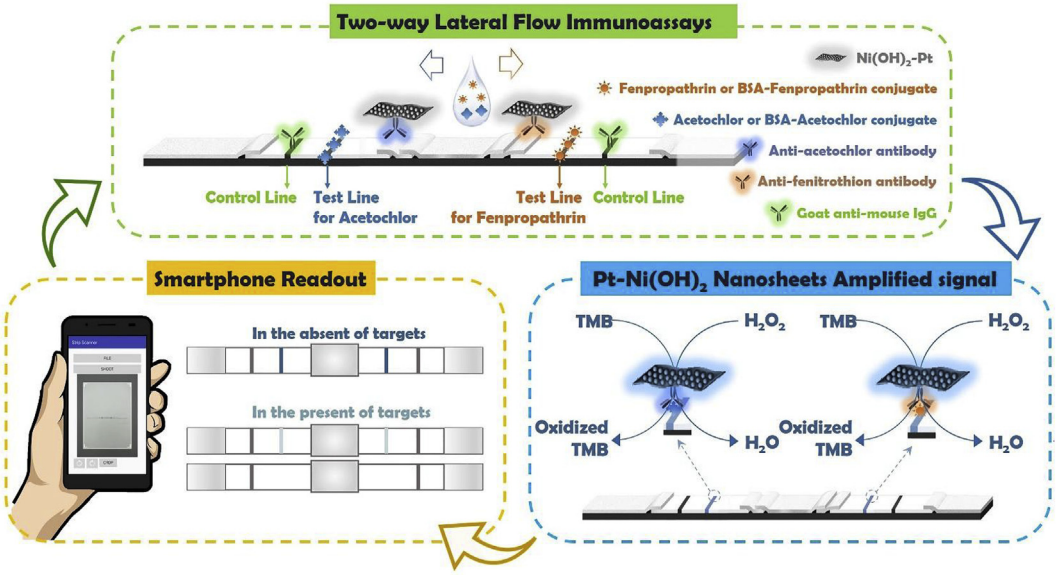

Scheme 1. Schematic diagram of two-way LFI for detection of acetochlor and fenpropathrin.

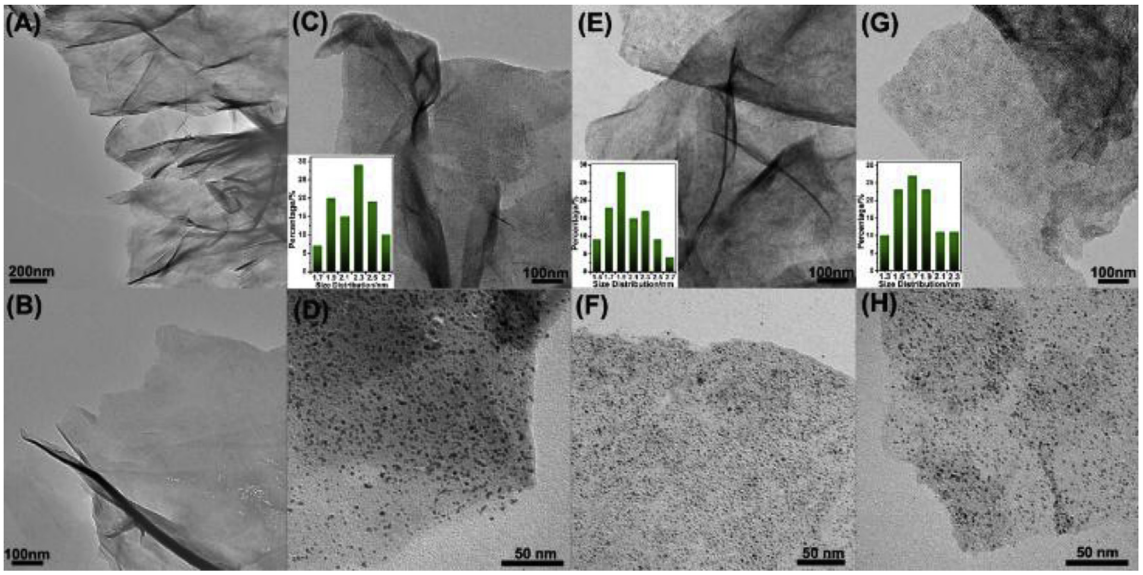

Fig. 1. Transmission electron microscopy (TEM) images of as-prepared $Ni(OH)_2$ nanosheets (A and B), $Ni(OH)_2$ nanosheets with Pt loading of 10% (C and D), 20% (E and F), and 40% (G and H), respectively. The insets in C, E and G are the size distribution of Pt nanoclusters.

(200) indicated by the green line were corresponding to Ni $(OH)_2{\cdot}0.75H_2O$ nanocrystals based on PDF# 38-0715. We also employed EDS for analyzing the composition of Pt-x/$Ni(OH)_2$ displayed in Fig. S1B, showing that there are apparently Pt and Ni peaks, evidencing the formation of Pt nanocrystals on $Ni(OH)_2$ nanosheets.

Catalytic reaction experiments were conducted to analyze and compare the HRP-like activity of the prepared Pt-10/$Ni(OH)_2$, Pt-20/Ni $(OH)_2$ and Pt-40/$Ni(OH)_2$ NSs. Typical images and response curves in Fig. S2 showed that Pt-10/$Ni(OH)_2$ NSs held the highest HRP-like activity, which could be attributed to the appropriate spatial density and larger size of Pt nanoclusters loaded on $Ni(OH)_2$ nanosheets. Thus, Pt-10/$Ni(OH)_2$ NSs were applied in the following residue detection experiments.

3.3. Optimization of the detection system

To achieve the best detection capability of the two-way LFI, we optimized various analytical parameters, including the amount of antibody modified Pt–$Ni(OH)_2$ NSs conjugates applied on the conjugate pad, the migration time of Pt–$Ni(OH)_2$ NSs on NC membrane, the loading mode of TMB and H_2O_2 mix solution, the reaction time for the immunoreactions, and the effect of different external light interference. As shown in Figs. 2A and 2.0 μL was the optimal amount of the applied antibody modified Pt–$Ni(OH)_2$ NSs conjugates because the peak area reached to maximum for 2.0 μL and then decreased after 3.0 μL. As depicted in Fig. 2B, the peak area increased with the migration time until 13 min, which was relatively longer compared with zero-dimensional nanoparticles due to the low migration speed of two-dimensional Pt–$Ni(OH)_2$ NSs. The effect of different loading modes of TMB and H_2O_2 mix solution was observed. Fig. 2C showed that directly loading TMB and H_2O_2 on the test lines (No. 4) resulted in good detection capability with weak background and enhanced signal. Therefore, this direct loading mode was used in our experiments. Finally, LFI images before and after signal enhancement were shown in Fig. 2D. The color of the test line changed to blue immediately after loading TMB and H_2O_2, which means excellent HRP-like activity of Pt–$Ni(OH)_2$ NSs even on NC membrane. Furthermore, the peak area remained stable for 10 min (data not shown). Therefore, LFI can be quantified within 10 min. To investigate the effect of different external light interference. Typical images and response relative peak areas were summarized in Fig. S3. The brilliant and moderate light exhibited similar signal output. The dark light showed higher signal output due to blurred boundaries, which may cause uncertainty error. In order to reduce the external light interference, the brilliant and moderate light are encouraged when using the smartphone-based detection system.

3.4. Semi-quantification by naked eyes

Under optimal experimental conditions, we simultaneously examined samples with different concentrations (from 0 to 200 ng/mL) of acetochlor and fenpropathrin using the prepared LFI and recorded the photograph to assess the performance of two-way LFI. Fig. 3 displays the typical photo image of the two-way LFI without (Fig. 3A) and with (Fig. 3B) enhancement by the TMB and H_2O_2 mix solution. We observed that the intensities of the two test lines were inversely related to the concentration of corresponding targets. Observing the image intensity by naked eye can obtain semi-quantitative information of the target concentration. Before enhancement, the saturation concentration was considered to be ~20 ng/mL. However, this value increased to ~200 ng/mL after enhancement, which was contributed by the enhanced effect on weak test lines. At the same time, the lowest visually detectable amount was imporved from ~1.0 ng/mL without single enhancement to ~0.1 ng/mL of targets with the enhancement, which was contributed by the amplificated effect on strong test lines. These results confirmed that the signal enhancement strategy can expand the detection range and improve the sensitivity effectively. Thus, the 2D Pt–Ni $(OH)_2$ NSs can be used as a novel enhanced label for herbicide and insecticide detection in our two-way LFI assay.

3.5. Quantification by portable smartphone-based system

In order to achieve smartphone-based readout, we developed a universal detection app, *Strip Scan*, based on Android system, which can be used for quantification of herbicide and insecticide continuously. The typical screen shoots of the app were shown in Fig. 4. This system integrated two image acquisition paths, “FILE” and “SHOOT”, which were displayed on the main menu. “FILE” allows the user to choose an image from an existing file for analysis, while “SHOOT” takes the image of the test lines from the LFI. Then, the user can select the concerned test line by narrowing the view range and convert the intensity of the line to the peak image by clicking on the “CROP”. After obtaining the corresponding peak image, the user can further narrow the view range

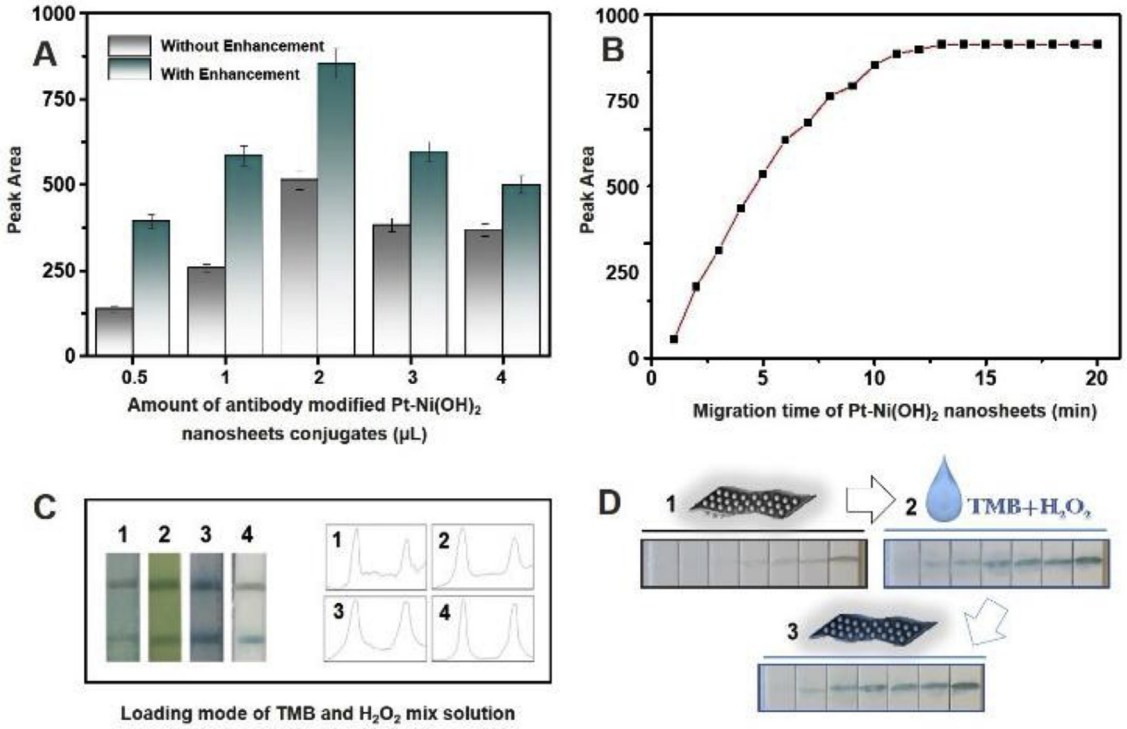

Fig. 2. Optimization of the detection system. (A) Effect of different amounts of antibody modified Pt–Ni(OH)$_2$ nanosheets conjugates on the conjugate pad. (B) Effect of different migration time of Pt–Ni(OH)$_2$ nanosheets on NC membrane. (C) Effect of different loading modes of TMB and H_2O_2 mix solution. (1) Partial immersion in the tube; (2) Totally immersion in tube; (3) Loading on sample pad; (4) Loading on the test line. (D) LFI images before and after signal enhancement. (1) LFI images before the signal enhancement; (2) LFI images when loading TMB and H_2O_2 mix solution immediately; (3) LFI images after the enhancement for 10 min.

to focus on the peak area. Subsequently, the concerned peak area values can be calculated and plotted by clicking the "FIRST" and "SECOND" buttons, which are in linear relationship with the concentrations of acetochlor and fenpropathrin, respectively. Then, we can calculate the concentrations of targets (unit: ng/mL) in the detected sample by entering the slopes and intercepts of the corresponding linear relationship into the app. The slopes and intercepts of both acetochlor and fenpropathrin are obtained from the corresponding pre-established standard curves. As shown in Fig. 5, there were obvious linear relationships between peak areas with the concentrations of acetochlor and fenpropathrin (acetochlor without enhancement over the 0.1–20 ng/mL range: $y = -9.5765x + 271.46$, $R^2 = 0.9982$; fenpropathrin without enhancement over the 0.1–20 ng/mL range: $y = -22.664x + 504.46$, $R^2 = 0.9932$; acetochlor with enhancement over the 1.0–150 ng/mL range: $y = -1.9533x + 317.97$, $R^2 = 0.9921$; fenpropathrin with enhancement over the 1.0–150 ng/mL range: $y = -3.6533x + 578.72$, $R^2 = 0.9913$). Finally, the calculated test results will be displayed on the cellphone screen. This design was the key to achieving universal detection using the proposed smartphone-based system. It should be noted that the limit of detection (LOD) of acetochlor and fenpropathrin were determined to be 0.63 ng/mL and 0.24 ng/mL based on 3.3 × standard deviation/slope, which was more sensitive than previous reported fluorescent biosensor, electrochemical biosensor or even chemiluminescence biosensor (Table S1). Thus, the 2D Pt–Ni(OH)$_2$ NSs as enhanced signal labels showed a high sensitivity based on their abilities for high HRP-like activity and low migration speed on NC membrane of LFIs.

3.6. Specificity

We investigated the specificity of the two-way LFI using some interfering herbicides and insecticides, such as chlorpyrifos, diazinon, malathion, atrazine and glyphosate, which were widely employed within the global agricultural community. Fig. S4 clearly showed that the proposed assay only responded to the corresponding targets, and the responses of other interfering herbicides and insecticides were

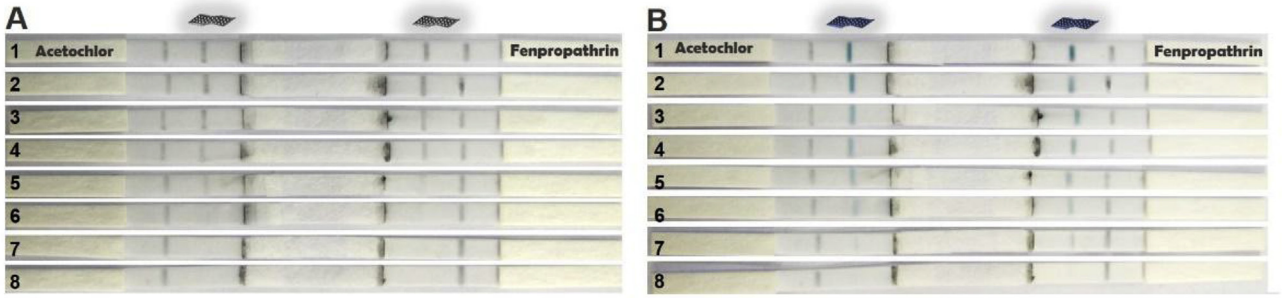

Fig. 3. Photograph of two-way LFIs for detection of acetochlor and fenpropathrin (A)without and (B) with the signal enhancement. Concentration of targets: (1) 0; (2) 0.1; (3)1.0; (4) 10; (5) 20; (6) 100; (7) 150; and (8) 200 ng/mL.

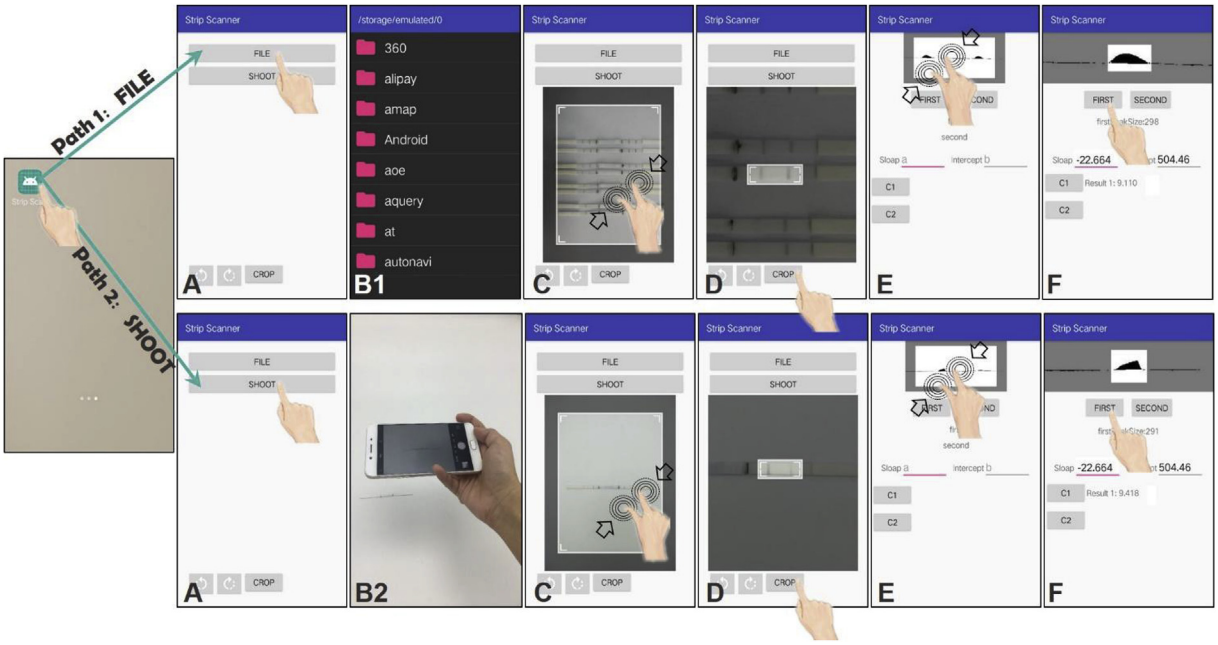

Fig. 4. Screenshots from the universal detection app named Strip Scan with two image acquisition paths for "FILE" and "SHOOT". (A) Choosing a path to acquire a photograph of two-way LFIs. (B1) Acquiring photograph from files. (B2) Acquiring a photograph from the camera. (C) Narrowing the view range until the view focuses on the concerned lines. (D) Clicking on "CROP" to convert the intensity of lines to the corresponding peak image. (E) Narrowing the view range to the concerned peak image. (F) Clicking on "FIRST" or "SECOND" to plot the peak area value and entering the slope and intercept of the corresponding linear relationship to calculate the test results (unit: ng/mL) of the detected sample.

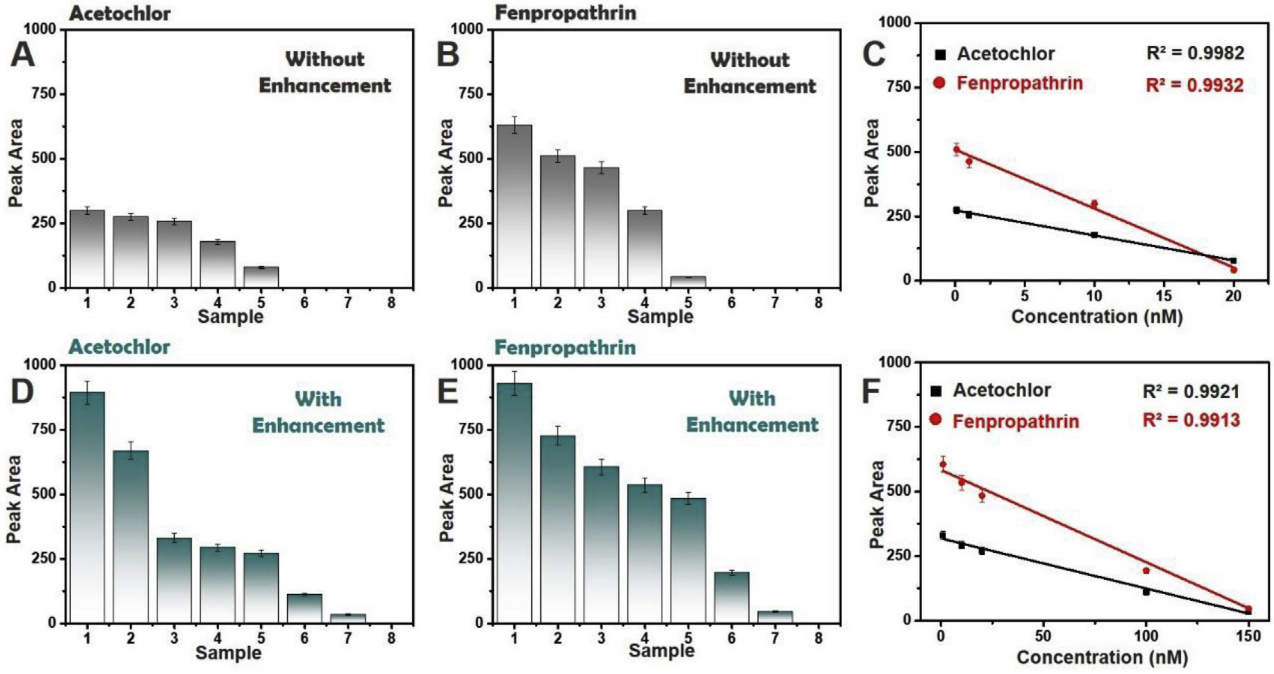

Fig. 5. The relationships between the peak area of test lines and different samples. (A) Plotted peak area in the response to various concentrations of acetochlor without enhancement. (B) Plotted peak area in the response to various concentrations of fenpropathrin without enhancement. (C) The standard curve of two-way LFIs for acetochlor and fenpropathrin detection without enhancement. (D) Plotted peak area in the response of various concentrations of acetochlor with enhancement. (E) Plotted peak area in the response of various concentrations of fenpropathrin with enhancement. (F) The standard curve of two-way LFIs for acetochlor and fenpropathrin detection with enhancement. Concentration of targets: (1) 0; (2) 0.1; (3)1.0; (4) 10; (5) 20; (6) 100; (7) 150; and (8) 200 ng/mL.

almost negligible. This result revealed the high specificity of the proposed system, which was associated with the novel design of two-way LFIs.

3.7. Detection of spiked samples

Detection of real food samples was performed using the proposed system. 10 non-spiked food samples, including corn, sorghum, soybean, apple, orange, peach, cabbage, broccoli, tomato, and drinking water

were first tested. All original samples showed "not detected" results of acetochlor and fenpropathrin measured by gas chromatography (NY/T 761-2008, agricultural industry standard of China) and the proposed method in this study. Furthermore, different concentrations of spiked samples (1.0 ng/mL, 10 ng/mL and 100 ng/mL) of corn, apple, and cabbage were prepared as matrix for spiked-recovery tests. The recovery rates were evaluated at between 97.12% and 111.46% for the proposed system in this study (Table S2). The data revealed the accuracy of the developed system and the feasibility of detection herbicide and insecticide in various matrixes, simultaneously.

4. Conclusion

In conclusion, we have developed a Pt–Ni(OH)$_2$ NSs amplified two-way LFI with smartphone readout for quantification of acetochlor and fenpropathrin. The core-technology of our proposed assay relies on the following aspects: (i) 2D Pt–Ni(OH)$_2$ NSs were synthesized via the facile and efficient microwave approach and used as enhanced signal label based on its advantageous properties of high HRP-like activity and low migration speed; (ii) two-way LFI was designed to eliminate cross-reaction between two targets; and (iii) a portable readout platform was developed based on a smartphone app, *Strip Scan*, with the advantage of universal data analysis. Overall, the multiplex, highly sensitive detection strategy developed in this study ensures a promising future in the field for rapid analysis of herbicides and insecticides.

Acknowledgment

This work is supported by the USDA National Institute of Food and Agriculture, AFRI project (2018-67021-27970).

Appendix A. Supplementary data

Supplementary data to this article can be found online at https://doi.org/10.1016/j.bios.2019.111498.

References

Cheng, N., Shang, Y., Xu, Y., Zhang, L., Luo, Y., Huang, K., Xu, W., 2017a. On-site detection of stacked genetically modified soybean based on event-specific TM-LAMP and a DNAzyme-lateral flow biosensor. Biosens. Bioelectron. 91, 408–416.

Cheng, N., Song, Y., Zeinhom, M.M.A., Chang, Y.-C., Sheng, L., Li, H., Du, D., Li, L., Zhu, M., Luo, Y., 2017b. Nanozyme mediated dual-immunoassay integrated with smartphone for use in simultaneous detection of pathogens. ACS Appl. Mater. Interfaces 9 (46), 40671–40680.

Duan, D., Fan, K., Zhang, D., Tan, S., Liang, M., Liu, Y., Zhang, J., Zhang, P., Liu, W., Qiu, X., 2015. Nanozyme-strip for rapid local diagnosis of Ebola. Biosens. Bioelectron. 74, 134–141.

Gao, X., Xu, L.-P., Wu, T., Wen, Y., Ma, X., Zhang, X., 2016a. An enzyme-amplified lateral flow strip biosensor for visual detection of MicroRNA-224. Talanta 146, 648–654.

Gao, Y., Deng, X., Wen, W., Zhang, X., Wang, S., 2016b. Ultrasensitive paper based nucleic acid detection realized by three-dimensional DNA-AuNPs network amplification. Biosens. Bioelectron. 92, 529–535.

Ge, X., Asiri, A.M., Du, D., Wen, W., Wang, S., Lin, Y., 2014. Nanomaterial-enhanced paper-based biosensors. Trac. Trends Anal. Chem. 58, 31–39.

He, Y., Zeng, K., Zhang, S., Gurung, A.S., Baloda, M., Zhang, X., Liu, G., 2012. Visual detection of gene mutations based on isothermal strand-displacement polymerase reaction and lateral flow strip. Biosens. Bioelectron. 31 (1), 310–315.

He, Z., Wang, L., Peng, Y., Luo, M., Wang, W., Liu, X., 2015. Multiresidue analysis of over 200 pesticides in cereals using a QuEChERS and gas chromatography–tandem mass spectrometry-based method. Food Chem. 169, 372–380.

Hou, Y., Wang, K., Xiao, K., Qin, W., Lu, W., Tao, W., Cui, D., 2017. Smartphone-based dual-modality imaging system for quantitative detection of color or fluorescent lateral flow immunochromatographic strips. Nanoscale Res. Lett. 12 (1), 291.

Jiang, T., Song, Y., Du, D., Liu, X., Lin, Y., 2016. Detection of P53 protein based on Pt-Pd nanoparticles with enhanced peroxidase-like catalysis. ACS Sensors 1 (6), 717–724.

Kiljanek, T., Niewiadowska, A., Semeniuk, S., Gaweł, M., Borzęcka, M., Posyniak, A., 2016. Multi-residue method for the determination of pesticides and pesticide metabolites in honeybees by liquid and gas chromatography coupled with tandem mass spectrometry—honeybee poisoning incidents. J. Chromatogr. A 1435, 100–114.

Kim, Y.A., Lee, E.-H., Kim, K.-O., Lee, Y.T., Hammock, B.D., Lee, H.-S., 2011. Competitive immunochromatographic assay for the detection of the organophosphorus pesticide chlorpyrifos. Anal. Chim. Acta 693 (1–2), 106–113.

Koo, C.K., He, F., Nugen, S.R., 2013. An inkjet-printed electrowetting valve for paper-fluidic sensors. Analyst 138 (17), 4998–5004.

Kwon, H., Chan, K.M., Kool, E.T., 2017. DNA as an environmental sensor: detection and identification of pesticide contaminants in water with fluorescent nucleobases. Org. Biomol. Chem. 15 (8), 1801–1809.

Lee, E.-H., Kim, Y.A., Lee, Y.T., Hammock, B.D., Lee, H.-S., 2013. Competitive immunochromatographic assay for the detection of the organophosphorus pesticide EPN. Food Agric. Immunol. 24 (2), 129–138.

Lee, J.-Y., Kim, Y.A., Kim, M.Y., Lee, Y.T., Hammock, B.D., Lee, H.-S., 2012. Importance of membrane selection in the development of immunochromatographic assays for low-molecular weight compounds. Anal. Chim. Acta 757, 69–74.

Li, N., Chen, J., Shi, Y.-P., 2015. Magnetic graphene solid-phase extraction for the determination of carbamate pesticides in tomatoes coupled with high performance liquid chromatography. Talanta 141, 212–219.

Liu, G., Wang, J., Barry, R., Petersen, C., Timchalk, C., Gassman, P.L., Lin, Y., 2008. Nanoparticle-based electrochemical immunosensor for the detection of phosphorylated acetylcholinesterase: an exposure biomarker of organophosphate pesticides and nerve agents. Chem. Eur J. 14, 9951–9959.

Martinez, A.W., Phillips, S.T., Carrilho, E., Thomas III, S.W., Sindi, H., Whitesides, G.M., 2008. Simple telemedicine for developing regions: camera phones and paper-based microfluidic devices for real-time, off-site diagnosis. Anal. Chem. 80 (10), 3699–3707.

Mudanyali, O., Dimitrov, S., Sikora, U., Padmanabhan, S., Navruz, I., Ozcan, A., 2012. Integrated rapid-diagnostic-test reader platform on a cellphone. Lab Chip 12 (15), 2678–2686.

Ouyang, H., Wang, W., Shu, Q., Fu, Z., 2018. Novel chemiluminescent immunochromatographic assay using a dual-readout signal probe for multiplexed detection of pesticide residues. Analyst 143 (12), 2883–28888.

Park, S., Kim, H., Paek, S.-H., Hong, J.W., Kim, Y.-K., 2008. Enzyme-linked immuno-strip biosensor to detect Escherichia coli O157: H7. Ultramicroscopy 108 (10), 1348–1351.

Roda, A., Michelini, E., Zangheri, M., Di Fusco, M., Calabria, D., Simoni, P., 2016. Smartphone-based biosensors: a critical review and perspectives. Trac. Trends Anal. Chem. 79, 317–325.

Rong-Hwa, S., Tang, S.S., Der-Jiang, C., Yao-Wen, H., 2010. Gold nanoparticle-based lateral flow assay for detection of staphylococcal enterotoxin B. Food Chem. 118 (2), 462–466.

Sajid, M., Kawde, A.-N., Daud, M., 2015. Designs, formats and applications of lateral flow assay: a literature review. J. Saudi Chem. Soc. 19 (6), 689–705.

Shu, Q., Wang, L., Ouyang, H., Wang, W., Liu, F., Fu, Z., 2017. Multiplexed immunochromatographic test strip for time-resolved chemiluminescent detection of pesticide residues using a bifunctional antibody. Biosens. Bioelectron. 87, 908–914.

Takalkar, S., Xu, H., Chen, J., Baryeh, K., Qiu, W., Zhao, J.X., Liu, A.G., 2015. Gold nanoparticle coated silica nanorods for sensitive visual detection of microRNA on a lateral flow strip biosensor. Anal. Sci. 32 (6), 617–622.

Wen, W., Song, Y., Yan, X., Zhu, C., Du, D., Wang, S., Asiri, A.M., Lin, Y., 2018. Recent advances in emerging 2D nanomaterials for biosensing and bioimaging applications. Mater. Today 21 (2), 164–177.

Yan, X., Li, H., Hu, T., Su, X., 2017. A novel fluorimetric sensing platform for highly sensitive detection of organophosphorus pesticides by using egg white-encapsulated gold nanoclusters. Biosensors and Bioelectronics 91, 232–237.

Xu, H., Ding, L.-X., Feng, J.-X., Li, G.-R., 2015. Pt/Ni (OH) 2–NiOOH/Pd multi-walled hollow nanorod arrays as superior electrocatalysts for formic acid electrooxidation. Chem. Sci. 6 (12), 6991–6998.

You, D.J., San Park, T., Yoon, J.-Y., 2013. Cell-phone-based measurement of TSH using Mie scatter optimized lateral flow assays. Biosens. Bioelectron. 40 (1), 180–185.

You, M., Lin, M., Gong, Y., Wang, S., Li, A., Ji, L., Zhao, H., Ling, K., Wen, T., Huang, Y., 2017. Household fluorescent lateral flow strip platform for sensitive and quantitative prognosis of heart failure using dual-color upconversion nanoparticles. ACS Nano 11 (6), 6261–6270.

Zhang, L., Chen, Y., Cheng, N., Xu, Y., Huang, K., Luo, Y., Wang, P., Duan, D., Xu, W., 2017. Rapid and ultra-sensitive detection of viable Enterobacter sakazakii by a continual cascade nanozyme biosensor. Anal. Chem. 89 (19), 10194–10200.

Zhang, W., Asiri, A.M., Liu, D., Du, D., Lin, Y., 2014. Nanomaterial-based biosensors for environmental and biological monitoring of organophosphorus pesticides and nerve agents. Trac. Trends Anal. Chem. 54, 1–10.